

Vertical extent of the newborn San Andreas fault at the Mendocino triple junction

J.A. Hole*

Department of Geological Sciences, Virginia Polytechnic Institute and State University, Blacksburg, Virginia 24061-0420, USA

B.C. Beaudoin

IRIS PASSCAL Instrument Center, New Mexico Institute of Mining and Technology, Socorro, New Mexico 87801, USA

S.L. Klemperer

Department of Geophysics, Stanford University, Stanford, California 94305, USA

ABSTRACT

Three-dimensional seismic refraction data reveal the structure of the plate boundaries at the Mendocino triple junction. First arrival traveltimes were inverted to obtain a three-dimensional seismic velocity model. The tomography results indicate a strong lateral velocity contrast in the lower crust. This velocity contrast is beneath the surface trace of the San Andreas fault and tracks along the fault to the triple junction and then along the Mendocino fracture zone. Velocity values appropriate for mafic rocks are more than 5 km shallower on the Pacific plate than east of the San Andreas fault, and 1–3 km shallower than under the Cascadia accretionary prism. The model suggests that the San Andreas fault, which is growing as the triple junction migrates northward, cuts steeply through the entire crust. Pacific oceanic crust does not extend beneath North America at this location. The slabless window south of the triple junction and east of the San Andreas fault must be filled with upwelling asthenosphere. The sharp corner of the Pacific plate migrates northward, displacing the Cascadia accretionary prism and forcing the prism material to move north or east.

Keywords: seismic tomography, California, plate boundary, San Andreas fault, Mendocino triple junction.

INTRODUCTION

The Mendocino triple junction in northern California is migrating northward, replacing the Cascadia subduction zone with the strike-slip San Andreas fault (Fig. 1). While the Pacific plate south of the Mendocino fracture zone has been adjacent to the strike-slip fault system since before 25 Ma, new San Andreas fault is being created in the North American crust. New three-dimensional seismic refraction data illuminate lower crustal structure of the three plates at the triple junction and constrain models for the evolution of the San Andreas fault.

The corner of the Pacific plate includes a wedge of felsic rocks, the Vizcaino block, that formed as an accretionary prism and was sliced off the continental margin some time after initiation of the strike-slip plate boundary (McLaughlin et al., 1994). Seismic refraction data indicate the presence of a layer beneath the Vizcaino block that has a high velocity indicative of mafic rocks, interpreted as oceanic crust (Henstock et al., 1997; Leitner et al., 1998; Henstock and Levander, 2000). The western margin of North America adjacent to the northernmost San Andreas fault consists of Tertiary accretionary prism rocks of the Franciscan terrane. A high-velocity mafic layer, similar to that offshore, is observed in the lower crust beneath the Franciscan terrane (Beaudoin et al., 1996, 1998; Henstock et al., 1997; Henstock and Levander, 2000). North of the triple junction, the active Cascadia accretionary prism overlies oceanic crust of the subducting Juan de Fuca plate.

As the subducted Juan de Fuca slab migrates northward, a slabless window is created beneath North America (Dickinson and Snyder, 1979). This window must be filled either by asthenospheric upwelling (e.g., Lachenbruch and Sass, 1980; Furlong, 1984), northward-migrating Pacific plate that extends beneath the continent (e.g., Bohannon and Parsons, 1995), or portions of the Juan de Fuca slab that do not subduct (e.g., ten Brink et al., 1999). In the first model, the mafic lower crust beneath North America was accreted to the base of the continent by magmatism derived from pressure-

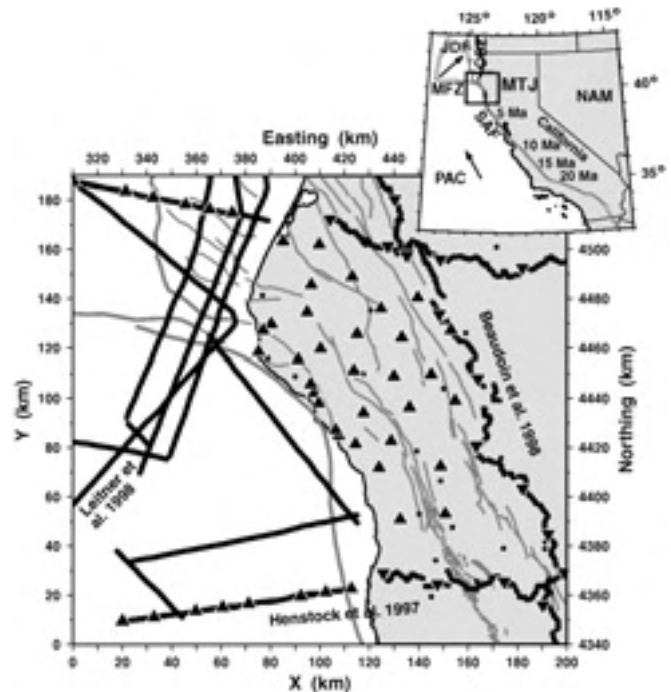


Figure 1. Map of Mendocino triple junction (MTJ) region, showing seismic sources and receivers used in three-dimensional tomography. Triangles are land or ocean-bottom seismographs that recorded offshore air-gun shots (lines). Inverted triangles are explosive shots recorded at onshore receivers (dots). Published refraction profiles are labeled. Faults are shown in gray; main plate-boundary faults are thicker. Index map shows plates and plate boundaries, directions of plate motion relative to North America (NAM), and locations of MTJ relative to NAM at indicated dates. PAC—Pacific plate; JDF—Juan de Fuca plate; SAF—San Andreas fault; MFZ—Mendocino fracture zone; CSZ—Cascadia subduction zone.

*E-mail: hole@vt.edu.

release melting of the upwelling asthenosphere. In the second model, the mafic rocks are oceanic crust attached to the Pacific plate. In the third model, the mafic rocks are oceanic crust of the Juan de Fuca plate attached to North America.

Seismic refraction data constrain the mafic layers to be at different depths on either side of the San Andreas fault at a location (Fig. 1) that was at the triple junction 2 m.y. ago (Henstock et al., 1997; Henstock and Levander, 2000). The observed sharp vertical offset in the mafic layer indicates that the San Andreas fault, which is not defined by modern seismicity, cuts vertically through the entire crust. This does not allow oceanic crust of the Pacific plate to extend across the San Andreas fault. Seismic refraction and gravity data indicate that the Juan de Fuca oceanic crust has a distinct southern edge inboard of the triple junction (Beaudoin et al., 1998), and is thus not extending to fill the entire slab gap.

THREE-DIMENSIONAL SEISMIC DATA

In 1993 and 1994, a seismic reflection and refraction survey sampled the Mendocino triple junction region (Fig. 1). Long-offset recordings of both marine airgun and land explosion sources were used to obtain seismic velocity structure of the crust. Data were recorded in an in-line geometry for onshore shots recorded on onshore seismographs and for airgun shots recorded on both ocean-bottom and land seismographs. These data constrain deep two-dimensional crustal structures across the plate boundaries (Henstock et al., 1997; Beaudoin et al., 1998; Gulick et al., 1998; Leitner et al., 1998). In addition, the offshore airgun shots were recorded by an array of onshore seismographs to obtain three-dimensional ray coverage of the triple junction (Fig. 1).

First-arrival traveltimes were picked for all source and receiver combinations in Figure 1. The data set represents 237 929 rays. Bathymetry and

sedimentary basin thickness and average velocity were obtained from the marine multichannel reflection data. The airgun shots were moved to basement using a shift in horizontal position, vertical position, and time. This shift used straight rays in the water column and in the sediment. Each ray pointed toward the receiver with a takeoff angle calculated from an apparent velocity of 6 km/s at source-receiver offsets <80 km and 8 km/s at greater offsets. These corrections removed large traveltimes delays due to the water and sediment and prevented mapping these delays into the deeper velocity model.

The traveltimes data were inverted using the tomography algorithm of Hole (1992) to obtain a three-dimensional velocity image. The model region of Figure 1 was sampled at a 1 km grid spacing. The two-dimensional onshore and ocean-bottom seismograph data were given 10 times weighting in the inversion because they provide the best short-offset constraints on upper crustal structure. The iterative, nonlinear inversion scheme was initiated with a huge smoothing operator of $140 \times 140 \times 14$ km, which was gradually reduced as the model converged. This scheme reduces dependence upon the starting model and produces a very smooth result containing only large-scale structure required by the data. The final smoothing operator was $40 \times 40 \times 4$ km. This result is intentionally underconverged to ensure that the three-dimensional structure is averaged over several receivers, and is thus less likely to be biased by local errors at shallow depth. The starting velocity model increased linearly with depth. Starting velocity models with very different gradients were tested, but produced very similar results for the large-scale features interpreted here. There was no attempt to incorporate realistic lateral velocity variations across the plate boundaries or discontinuities above the lower crust and mantle; the goal was to determine whether the data require these features. Spatial resolution is ~ 30 km horizontally and ~ 3 km vertically. Differences in velocity structure are better defined than absolute velocity or depth values.

THREE-DIMENSIONAL VELOCITY MODEL

Figure 2 shows cross sections through the velocity model across the major plate boundaries. Velocity values in the upper crust are <6 km/s, characteristic of the Franciscan and younger accretionary prism rocks. Minor velocity contrasts exist across the plate boundaries in the upper crust. Velocities increase to ~ 7 km/s in the lower crust, indicative of mafic rocks.

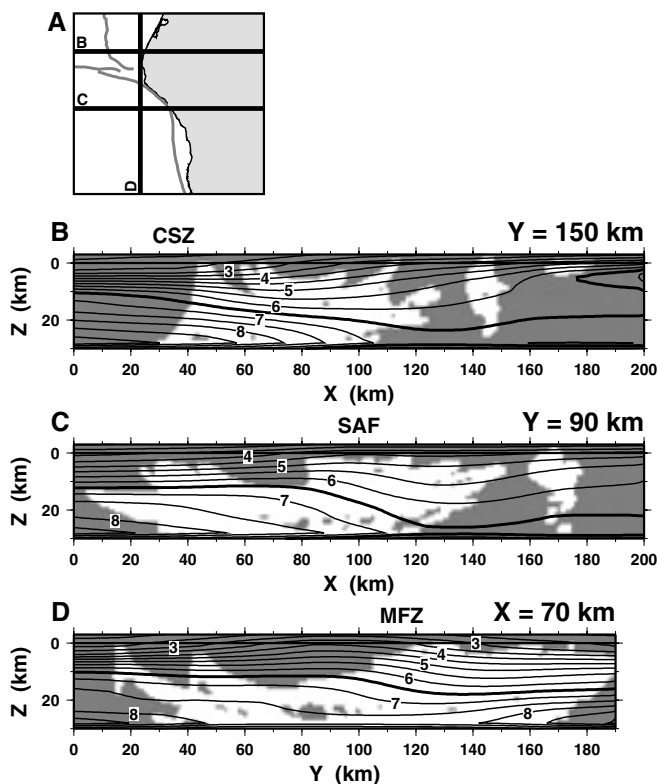


Figure 2. Contoured cross sections through three-dimensional tomography model, labeled in kilometers per second. 6.5 km/s contour is thicker, representing smoothed approximation to felsic-mafic discontinuity. Regions >1 km from rays are shaded gray. Surface locations of plate-boundary faults are labeled as in Figure 1. Note that cross-section D is perpendicular to B and C. Abbreviations as in Figure 1.

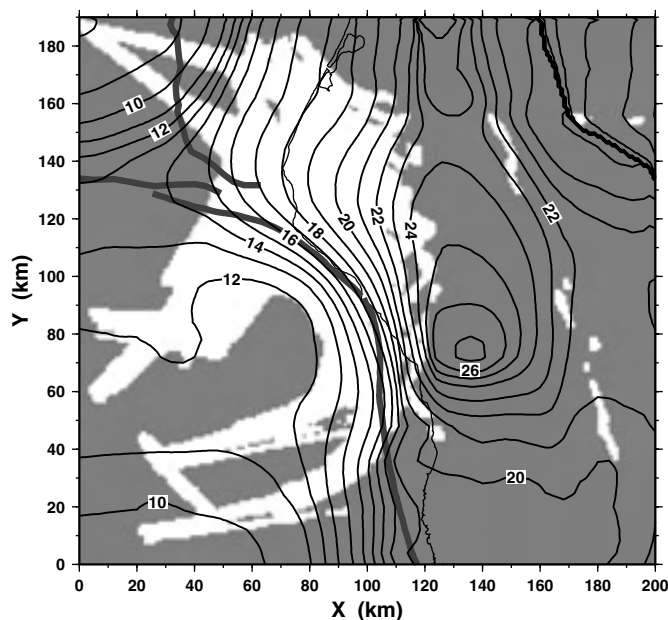


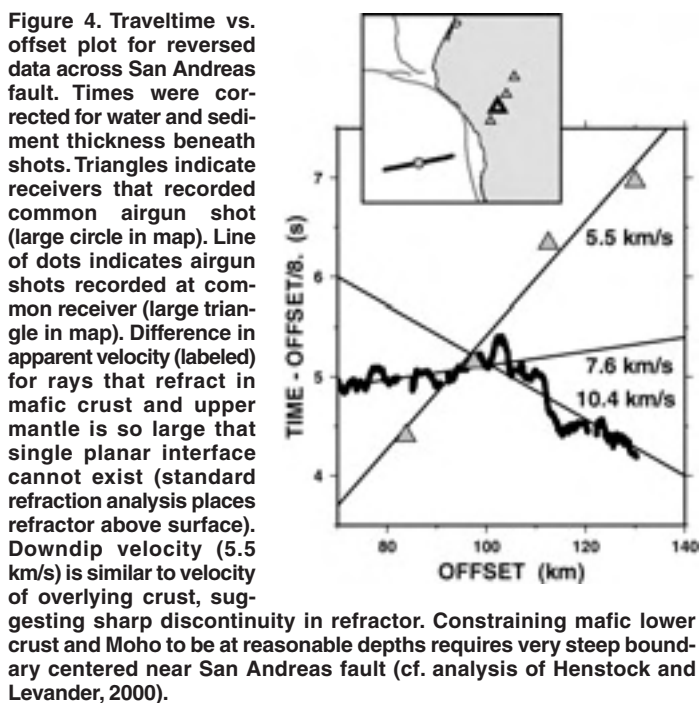
Figure 3. Contour map, in kilometers, of depth at which 6.5 km/s is encountered in three-dimensional velocity model. Regions >1 km from rays are shaded gray. Surface locations of coast and plate-boundary faults are shown.

The true sharp discontinuity, identified by the two-dimensional studies, between the felsic upper crust and mafic lower crust is smoothed vertically in the model. A strong lateral velocity contrast is observed in the lower crust centered under the San Andreas fault and Mendocino fracture zone (Fig. 2). Near these transform faults, mafic velocity is encountered several kilometers shallower in the Pacific plate than in the North American plate or Cascadia accretionary prism.

In order to show the top of the mafic lower crust, Figure 3 is a map of depth to a velocity of 6.5 km/s, intermediate between felsic and mafic values. The depth at 6.5 km/s dips smoothly beneath the Cascadia subduction zone and is similar to the top of the oceanic Juan de Fuca crust (Beaudoin et al., 1994, 1996; Gulick et al., 1998). The depth to 6.5 km/s dips shallowly eastward on the Pacific plate. Mafic velocities are poorly constrained by the data set beneath North America except along the north-south profile, but must be deeper than 20 km. The map shows a steep slope centered under the surface trace of the San Andreas fault and curving around the triple junction and along the Mendocino fracture zone. Due to smoothing, the inversion will underestimate sharp structures. The true dip of the top of the mafic layer is probably steeper and could be vertical beneath the transform faults. This result agrees with Henstock et al. (1997) and Henstock and Levander (2000), who indicated a 4 km vertical offset beneath the San Andreas fault in the southern portion of the study area (Fig. 1).

Two simple tests were performed to verify the steep offset across the San Andreas fault. Figure 4 shows traveltime picks for an airgun shot recorded on several onshore receivers and for a receiver recording numerous airgun shots. These data provide reversed refraction times from the lower crust under the San Andreas fault. The apparent velocity of the airgun shot gather is much lower shooting down dip than that of the receiver gather shooting up dip. The extreme difference in apparent velocity cannot be matched by a single planar refracting interface, but requires an interface that is steepened near the San Andreas fault.

Figure 5 shows the model and results of a synthetic test to determine whether the steep top of the lower crust could be an artifact of a poorly mapped lateral variation across the San Andreas fault in the upper crust. Synthetic traveltime data were computed for a velocity model that contains realistic values but imposes a strong lateral velocity contrast in the upper crust across the San Andreas fault and Mendocino fracture zone. The North



American velocity is slower than the Pacific, consistent with a traveltime delay that might make the lower crust appear deeper. The mafic layer in the lower crust is undeformed beneath the San Andreas fault (Fig. 5). While absolute depths are not accurate, tomography recovers the smoothly dipping top of the Juan de Fuca mafic crust and the offset beneath the Mendocino fracture zone (Fig. 5). The lateral contrast in the upper crust creates an artificial steepening of the mafic layer beneath the San Andreas fault (Fig. 5). The synthetic lateral velocity contrast in the upper crust is at least 3 times stronger than realistic values of 0.0–0.3 km/s (Beaudoin et al., 1998; Leitner et al., 1998; Henstock and Levander, 2000). Despite this, the artificially steepened mafic layer in the synthetic test has less than half the slope of that recovered from the true data (cf. Figs. 5 and 3). The steep dip observed beneath the true San Andreas fault is not an artifact of unmodeled shallower structure. In addition, the vertical offset across the synthetic Mendocino fracture zone (Fig. 5B) is smoothed by the inversion across a distance very similar to the steep slopes observed beneath the true Mendocino fracture zone and San Andreas fault (Fig. 3). This suggests that these features are probably very steep or vertical.

TECTONIC IMPLICATIONS

The tomography model indicates that there is a steep slope on the top of the mafic layer beneath the San Andreas fault and Mendocino fracture zone. We interpret this slope to be a smoothed image of a near-vertical offset, such that a mafic layer exists within all three plates, but is at different depths on either side of the plate-bounding faults. At the Mendocino frac-

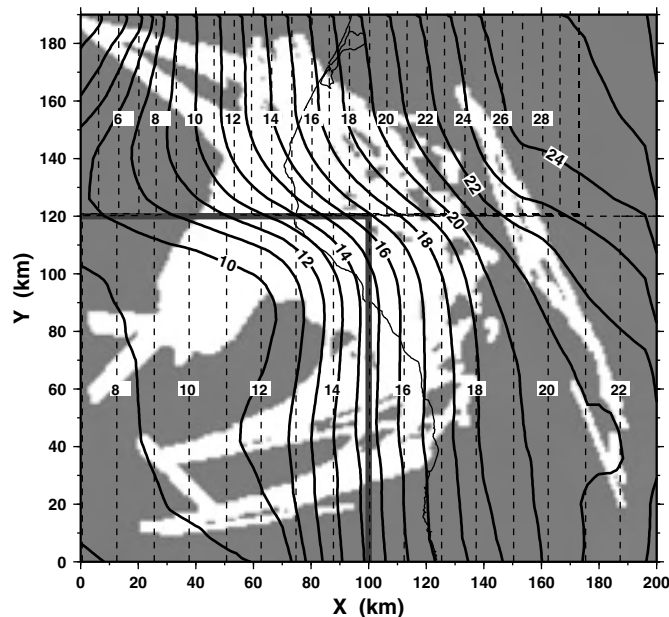


Figure 5. Contour map, in kilometers, of depth at which 6.5 km/s is encountered in synthetic velocity model (dashed lines) and resulting tomography model (solid lines). Synthetic model is composed of felsic upper crust (<6 km/s), mafic lower crust (7 km/s), and mantle (8 km/s). Gray lines indicate location of lateral velocity contrast of 1.0 km/s in upper crust; Pacific plate is faster. Model contains mafic lower crust that dips continuously beneath Cascadia subduction zone at depth similar to subducting Juan de Fuca plate. South of synthetic Mendocino fracture zone and its onshore extension, different mafic layer dips to east at angle shallower than to north. This layer is undisturbed beneath synthetic San Andreas fault. Moho is parallel to top of mafic layers and is 6 km deeper. Source-receiver geometry of real data was used to create synthetic traveltime data. Tomography model was derived from synthetic data using procedure identical to that for real data. Upper crustal velocity model was moderately well recovered, but lateral velocity contrast was smoothed by ~30 km. Mafic layer is artificially steepened beneath San Andreas fault, but dips much less than that observed in real data. Regions >1 km from rays are shaded gray.

ture zone, the mafic layers on either side are oceanic crust of different ages juxtaposed across a vertical fault. The Juan de Fuca crust is shallower than the Pacific crust at the western edge of the study area, consistent with Leitner et al. (1998), but becomes deeper than the Pacific toward the triple junction. A similar interpretation of the mafic layers is required across the San Andreas fault: the fault cuts vertically through the entire crust. This extends the results of Henstock et al. (1997) from a location where the age of the San Andreas fault is ca. 2 Ma to the triple junction at 0 Ma.

Oceanic crust of the Pacific plate does not extend across the San Andreas fault at this latitude as proposed by Bohannon and Parsons (1995). Along the profile at the eastern edge of the study area (Fig. 1), Beaudoin et al. (1998) located the southern edge of the subducted Juan de Fuca slab. The Juan de Fuca crust does not extend far south of the triple junction as proposed by ten Brink et al. (1999). These observations require that upwelling asthenosphere filled the window in the slab east of the San Andreas fault immediately after passage of the Mendocino triple junction. The mafic layer east of the San Andreas fault is either material attached to the continent prior to passage of the triple junction or material that was accreted to the base of the continent by magmatism after passage of the triple junction (Hole et al., 1998). Beaudoin et al. (1998) observed an ~40 km gap without mafic rocks south of the subducted slab and interpreted the gap to represent the region where upwelling and magmatism are currently active within the slabless window. The adjacent deep pit in the depth to 6.5 km/s (Fig. 3) may indicate that the mafic layer is absent, rather than deep, consistent with this interpretation.

The tomography results confirm that the location of the northeastern corner of the Pacific plate is much farther east than the Cascadia trench and extends vertically through the entire crust. The modern accretionary prism north of the triple junction must be displaced by the Pacific plate as it moves northward. The volume that must be removed is a triangle in cross section that is ~60 km in east-west extent and ~15 km thick at its eastern end. The >15 km thickness of North American crust east of the San Andreas fault suggests that the current geometry also existed in the past. Some of the Cascadia accretionary prism may be pushed to the east of the San Andreas fault as the triple junction passes, but uplift rates of the Franciscan are not consistent with accommodation of the entire volume (e.g., Merritts and Bull, 1989). Recent data indicate that the sediments on top of the corner of the Pacific plate are older than 11 Ma and that the Vizcaino block was attached to the Pacific plate when the sediments were deposited (Godfrey et al., 1998). Thus the Cascadia prism is not falling onto the Pacific plate. The only other direction that the prism can move is northward along the coast. Geodetic data suggest that the coast of Oregon is moving northward 10–15 mm/yr (McCaffrey et al., 1999), consistent with this model. Although major dextral strike-slip faults are not known in the subduction complex, oblique slip distributed on several thrust faults could take up the northward motion.

Three-dimensional tomography at the Mendocino triple junction has revealed that the corner of the Pacific plate has vertical edges that extend through the entire crust. This observation confirms the most simple model of plate interactions at the triple junction, and contradicts models that extend the Pacific plate beneath North America.

ACKNOWLEDGMENTS

The seismic data were acquired by scientists at Oregon State, Lehigh, Rice, and Stanford Universities, and the U.S. Geological Survey (USGS) using funding from the National Science Foundation Continental Dynamics Program. Facilities included the R/V *Ewing* and R/V *Wecoma*, and seismographs from IRIS-PASSCAL, the U.S. Geological Survey, and the Geological Survey of Canada. Traveltimes from two-dimensional data were provided by Anne Trehu. Offshore sediment thickness data were provided by Anne Meltzer and Amy Ondrus. Data analysis was funded by the National Earthquake Hazards Reduction Program of the U.S. Geological Survey. Beaudoin and Hole initiated this project at Stanford University.

REFERENCES CITED

- Beaudoin, B.C., Magee, M., and Benz, H., 1994, Crustal velocity structure north of the Mendocino triple junction: *Geophysical Research Letters*, v. 21, p. 2319–2322.
- Beaudoin, B.C., Godfrey, N.J., Klemperer, S.L., Lendl, C., Trehu, A.M., Henstock, T.J., Levander, A., Holl, J.E., Meltzer, A.S., Luetgert, J.H., and Mooney, W.D., 1996, Transition from slab to slabless: Results from the 1993 Mendocino triple junction seismic experiment: *Geology*, v. 24, p. 195–199.
- Beaudoin, B.C., Hole, J.A., Klemperer, S.L., and Trehu, A.M., 1998, Location of the southern edge of the Gorda slab and evidence for an adjacent asthenospheric window: Results from seismic profiling and gravity: *Journal of Geophysical Research*, v. 103, p. 30,101–30,115.
- Bohannon, R.G., and Parsons, T., 1995, Tectonic implications of post-30 Ma Pacific and North American relative plate motions: *Geological Society of America Bulletin*, v. 107, p. 937–959.
- Dickinson, W.R., and Snyder, W.S., 1979, Geometry of subducted slabs related to San Andreas transform: *Journal of Geology*, v. 87, p. 609–627.
- Furlong, K.P., 1984, Lithospheric behavior with triple junction migration: An example based on the Mendocino triple junction: *Physics of the Earth and Planetary Interiors*, v. 36, p. 213–223.
- Godfrey, N.J., Meltzer, A.S., Klemperer, S.L., Trehu, A.M., Leitner, B., Clarke, S.H., Jr., and Ondrus, A., 1998, Evolution of the Gorda Escarpment, San Andreas fault, and Mendocino triple junction from multichannel seismic data collected across the northern Vizcaino block, offshore northern California: *Journal of Geophysical Research*, v. 103, p. 23,813–23,825.
- Gulick, S.P.S., Meltzer, A.M., and Clarke, S.H., Jr., 1998, Seismic structure of the southern Cascadia subduction zone and accretionary prism north of the Mendocino triple junction: *Journal of Geophysical Research*, v. 103, p. 27,207–27,222.
- Henstock, T.J., and Levander, A., 2000, Lithospheric evolution in the wake of the Mendocino triple junction: Structure of the San Andreas fault system at 2 Ma: *Geophysical Journal International*, v. 140, p. 233–247.
- Henstock, T.J., Levander, A., and Hole, J.A., 1997, Deformation in the lower crust of the San Andreas fault system in northern California: *Science*, v. 278, p. 650–653.
- Hole, J.A., 1992, Nonlinear high-resolution three-dimensional seismic travel time tomography: *Journal of Geophysical Research*, v. 97, p. 6553–6562.
- Hole, J.A., Beaudoin, B.C., and Henstock, T.J., 1998, Wide-angle seismic constraints on the evolution of the deep San Andreas plate boundary by Mendocino triple junction migration: *Tectonics*, v. 17, p. 802–818.
- Lachenbruch, A.H., and Sass, J.H., 1980, Heat flow and energetics of the San Andreas fault zone: *Journal of Geophysical Research*, v. 85, p. 6185–6222.
- Leitner, B., Trehu, A.M., and Godfrey, N.J., 1998, Crustal structure of the northwestern Vizcaino block and Gorda Escarpment, offshore northern California, and implications for postsubduction deformation of a paleoaccretionary margin: *Journal of Geophysical Research*, v. 103, p. 23,795–23,812.
- McCaffrey, R., Goldfinger, C., Stevens, C.W., Johnson, C.K., Zwick, P., Long, M., Williams, C., Johnson, J., Zhou, Y., Nabelek, J., Murray, M.H., and Smith, C.L., 1999, GPS measurements of plate coupling and strain partitioning in northwestern Oregon: *Eos (Transactions, American Geophysical Union)*, v. 80, fall meeting supplement, p. F267.
- McLaughlin, R.J., Sliter, W.V., Frederiksen, N.O., Harbert, W.P., and McCulloch, D.S., 1994, Plate motions recorded in tectonostratigraphic terranes of the Franciscan complex and evolution of the Mendocino triple junction, northwestern California: *U.S. Geological Survey Bulletin* 1997, 60 p.
- Merritts, D., and Bull, W.B., 1989, Interpreting Quaternary uplift rates at the Mendocino triple junction, northern California, from uplifted marine terraces: *Geology*, v. 17, p. 1020–1024.
- ten Brink, U.S., Shimizu, N., and Molzer, P.C., 1999, Plate deformation at depth under northern California: Slab gap or stretched slab?: *Tectonics*, v. 18, p. 1084–1098.

Manuscript received May 23, 2000

Revised manuscript received September 5, 2000

Manuscript accepted September 14, 2000